Neurology Asia 2015; 20(2) : 143 – 153

Volume estimation of the subcortical structures in Parkinson's disease using magnetic resonance imaging: A methodological study

[1]Tolga Ertekin, [1]Niyazi Acer, [2]Semra İçer, [3]Ümit Erkan Vurdem, [4] Şerife Çınar, [5]Özlem Özçelik

[1]Department of Anatomy, Medical Faculty, Erciyes University, Kayseri; [2]Department of Biomedical Engineering, Engineering Faculty, University of Erciyes, Kayseri; [3]Department of Radiology, Kayseri Training and Research Hospital, Kayseri; [4]Ivrindi Health Care Vocational Schools, Balıkesir University, Balıkesir; [5]Nevşehir Hacı Bektaş Veli University, Semra and Vefa Küçük Health College, Nevşehir, Turkey

Abstract

Background & Objectives: Parkinson's disease (PD) is the most prevalent neurodegenerative disorder, beginning in the in the substantia nigra and spreading to the subcortical structures to the limbic cortices, and eventually to the neocortex and is characterized clinically by tremor at rest, bradykinesia, and rigidity. Regional brain atrophy is found to be an important marker of PD's pathology. The aim of the current study was to compare the volumes of subcortical brain structures between healthy subjects and patients with PD using stereological (point-counting) and semi-automated segmentation methods. *Methods:* Twenty-four patients with PD and 23 age matched healthy subjects free of any psychiatric, neurological or cognitive impairment were included in our study. Magnetic resonance images were analyzed by using two methods. *Results:* Both methods showed a decrease in volume of caudate nucleus and lentiform nucleus in PD group compared to the control group. ($p<0.05$). However, no significant differences was found between patient and control groups for the volume of thalamus ($p>0.05$)**.** Also, no significant difference was found between point-counting and semi-automated segmentation methods for the volumes of subcortical structures in both two groups ($p>0.05$)**.**
Conclusion: Magnatic resonance imaging is helpful to facilitate the diagnosis in vivo of patients with PD, revealing atrophy of specific brain regions such as caudate nucleus and lentiform nucleus.

INTRODUCTION

Parkinson's disease (PD) is a neurodegenerative, chronic neurological disorder which shows symptoms such as rigidity, tremor and bradykinesia and affects central and enteric nervous system.[1] Gradual degeneration of dopaminergic neurons in the pars compacta of substantia nigra is one of the earliest pathological feature of PD. Later, the disease pathological process gradually spreads from the subcortical structures to the limbic cortices, and eventually to the neocortex leading to structural abnormalities.[2]

Atrophy is thought to be a marker of neurodegenerative pathology.[3] The different features of PD (e.g., akinesia and tremor) are explained by deterioration of the motor basal ganglia circuits between cortex, striatum, pallidum to thalamus, and thalamus to cortex. They are essential foci for the development of the symptomatology of PD.[4] Measures of regional brain volumes, which can be derived from magnetic resonance imaging (MRI) images by dividing a brain into its constituent parts, can be used as structural indicators of many different neuropsychiatric disorders, such as schizophrenia, PD, and Alzheimer's disease.[5-7] MRI is thought to be able to facilitate the diagnosis in vivo of patients with PD revealing either signal changes or atrophy of specific brain regions.[8] Manual, semi-automated and automated methods were used in recent studies related to MR volumetric measurements of subcortical structures.[6,7,9,10] The analysis of subcortical volumes in patients with PD is essential to identify changes related to disease processes. Several volumetric studies have been performed to characterize regional brain volume differences in PD. However, these structural brain imaging studies provided contradictory results.[11,12]

Address Correspondence to: Tolga Ertekin, PhD**,** Associate Professor, Department of Anatomy, University of Erciyes, School of Medicine, Kayseri,38039, Turkey. Tel: 00 90 505 6482854, Fax: 00 90 352 437 52 85, e-mail: tolga.ertekin@yahoo.com.tr

Thus, a detailed knowledge on the subcortical structures and changes in this morphology related with PD may be of importance for reliable diagnoses. The value of our study lies in the fact that only few studies in the literature have investigated the volume of basal nuclei using stereological method and to the best of our knowledge, there is no study to compare between stereological and segmentation methods on patients with PD. This study was designed to fill this gap in knowledge. We compared the volumes of subcortical brain structures such as caudate nucleus, lentiform nucleus (globus pallidus+putamen) and thalamus using stereological (point-counting) and semi-automated segmentation methods.

METHODS

Subjects

MRI from 24 patients with PD (mean age 66.66±10.68), 23 healthy age- matched controls (62.56±8.76) were obtained in Department of Radiology of Kayseri Education and Research Hospital. Control subjects were matched with patients on the basis of gender and age. There is no difference between two genders ($p>0.05$). All control subjects were healthy volunteers with no history of major psychiatric, neurological or cognitive impairment. Firstly, all images were evaluated by a radiologist to detect the presence of features typically occurring in PD, and to exclude abnormal signs in controls. All participants gave their written informed consent to participate in the study, which was approved by the local ethics committee.

MRI protocol

All MRI scans were acquired with a 1.5 Tesla MRI machine (GE Medical Systems Signa, HDI, France). Thin section MRI data were obtained using an axial 3D T_1-weighted Spoiled Gradient Recalled Echo (SPGR) sequence. The following parameters were used for the imaging proces for TR/TE: 12.3/5.1 ms, FOV: 21x21 cm, 2 mm slice thickness without gap, matrix: 256x192, flip angle: 8º and NEX: 1.59. The subcortical brain structures' contours were determined in T_1-weighted axial imaging for volume estimation.

Volume estimation techniques

(a) Point counting method

Point-counting method is based on the Cavalieri principle. An unbiased estimate of the volume of a structure is produced by summing cross-sectional areas on equally spaced parallel planes and multiplying the sum by the distance between adjacent planes according to Cavalieri's theorem.[13] For this measurement to be unbiased, the position of the first slice must be uniformly randomly started along the axis perpendicular to the planes. Also, stereologic volume estimation is optimized by "slicing" the object to be measured in the same orientation relative to each participant's anatomy.[14,15]

According to this method, we used 1 mm section thickness to estimate the region of interest (ROI) volume. The films were displayed on computer and the transparent square grid test system with d = 0.4 cm between the test points was superimposed, randomly covering the entire image frame (Figure 1). The points hitting the ROI sectioned surface area were counted for each section and the volumes of subcortical structures were estimated using the modified formula (Eq. 1) for volume estimations of radiological images shown below.[16]

$$V(PC) = T \times \left[\frac{SU \times d}{SL}\right]^2 x \Sigma P$$

where 'T' is the section thickness, 'SU' the scale unit of the printed film, '*d*' the distance between

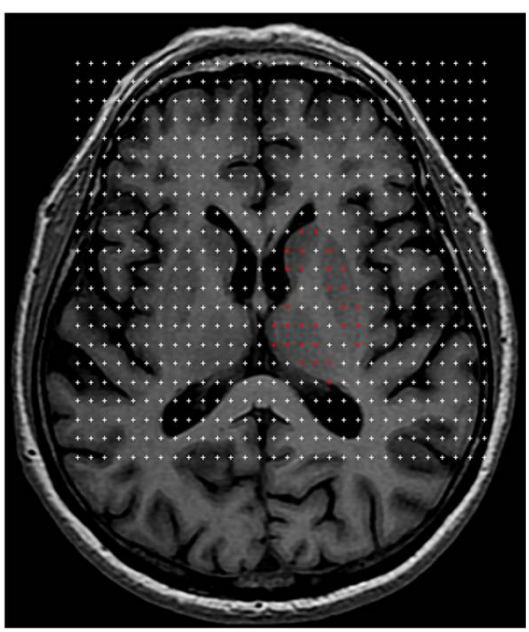

Figure 1. An axial MRI with a point-counting grid superimposed on it for the volume estimation of subcortical structures. Red points hitting the ROI sectioned surface area were counted for each section

the test points of the grid, 'SL' the measured length of the scale printed on the film and ΣP' is the total number of points hitting the sectioned cut surface areas of the subcortical structures.

Error prediction for point-counting

The coefficient of error (CE) of the point-counting method was calculated using the formula described in previous studies.[17,18] A CE value lower than 5% is in the acceptable range according to the literature.[19] It is also important to note that an appropriate grid size and the number of slices required for volume estimation of an object is crucial at the beginning.

(b) Segmentation of subcortical structures

This section focuses on the volume estimation and extraction of subcortical structures from the MR brain images. The proposed segmentation algorithm takes advantage of simple and powerful image processing techniques. Because the MR brain images are highly inhomogenity, (i.e. the contrast variety between the brain tissues) contrast enhancement is utilised. Other techniques such as h-minima transform and multilevel thresholding are exploited to decrease the number of intensity levels as much as possible, for making the subsequent threshold selection easier. Stages of the algorithm can be explained as follows, and can be summarized as shown in Figure 2.

1. Contrast enhancement

In the first step of the pre-processing stage, contrast enhancement is necessary to deepen the contrast of these images to provide a better transform representation for subsequent image analysis steps. In the proposed segmentation algorithm, histogram equalisation are exploited to perform the contrast enhancement.[20]

2. H-minima transform

Regional minima are connected components of pixels with a constant intensity value, and whose external boundary pixels all have a higher value. H-minima transform, all minima whose depth is lower than or equal to the given h-value are suppressed. The H-minima transform is a powerful mathematical tool to suppress undesired minima. Performing the H-minima transform on the inverse distance image can effectively decrease oversegmentation.[21]

3. Multilevel thresholding

In the proposed algorithm, multilevel thresholding technique is used to prepare the image for the binarisation process efficiently. The multilevel thresholding process helps in selecting the threshold value easily and more accurately. Multilevel thresholding is one of the most important image segmentation techniques, which converts the grey-scale image to an indexed image by decreasing the number of intensity levels.[22] In our study, the grey-scale levels are decreased to four levels to produce an image in which the threshold value for binarisation can be selected easily, as illustrated in Figure 2 (a).

4. Edge detection

Edge detection is the name for a set of mathematical methods which aim at identifying points in a digital image at which the image brightness changes sharply or, more formally, has discontinuities. The points at which image brightness changes sharply are typically organized into a set of curved line segments termed edges.[23] The edge detection results in segmentation algorithm of subcortical structures were shown on the Figure 2 (b). Thus, the areas of subcortical regions specified borders subcortical regions were determined as semi-automatically as shown Figure 2 (c-d).

Statistical analysis

The means and standard deviations (SDs) are presented. Statistical analysis was performed with SPSS 15.00 (SPSS, Chicago, IL, USA). Normality of distribution was tested using the Kolmogorov–Smirnov test and normal plot. We used Pearson correlation test to determine the degree of correlation between the subcortical structures. The differences in the mean volumes of the subcortical structures between groups were measured using the independent t test. Cavalieri and semi-automated segmentation methods comparison were tested using paired t test and Bland-Altman analysis. The accepted significance level was $p<0.05$.

RESULTS

In this study, we analyzed caudate nucleus, lentiform nucleus and thalamus volumetric differences between PD patients and control subjects by using stereologic and semi-automatic segmentation methods.

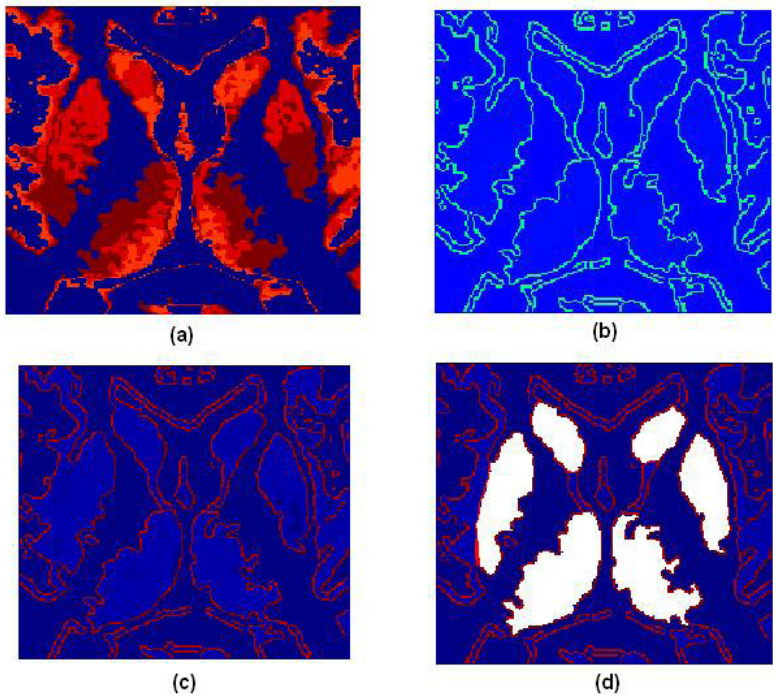

Figure 2. The segmentation steps of subcortical structures, (a) H-minima transform and Multilevel tresholding, (b) Edge detection, (c) sum of the (a) and (b), (d) segmentation of subcortical regions as semi-automatically

Table 1: Results of subcortical structures' volumes using point-counting and semi-automated segmentation techniques in both groups (cm^3), *p<0.05.

	Stereologic (mean±SD)			**Semi-automatic segmentation (mean±SD)**		
	Parkinson's Group (n=24)	Control Group (n=23)	P value	Parkinson's Group (n=24)	Control Group (n=23)	P value
Caudate nucleus	3.78±0.89	4,42±0.82	**0.013***	3.88±0.90	4.44 ± 0.64	**0.019***
Lentiform nucleus	6.40±1.55	7.52±1.14	**0.008***	6.52±1.38	7.43 ± 0.87	**0.011***
Thalamus	9.58±0.92	9.59±1.49	0.993	9.39±0.90	9.39 ±1.17	0.995
Caudate nucleus right	1.90±0.47	2.25±0.39	**0.009***	1,96±0.47	2.26±0.32	**0.016***
Caudate nucleus left	1.87±0.43	2.17±0.49	**0.031***	1.91±0.45	2.18±0.32	**0.027***
Lentiform nucleus right	3.23±0.76	3.87±0.56	**0.002***	3.28±0.66	3.78±0.45	**0.005***
Lentiform nucleus left	3.17±0.81	3.65±0.61	**0.029***	3.24±0.73	3.64±0.45	**0.03***
Thalamus right	4.86±0.50	4.89±0.70	0.855	4.78±0.44	4.79±0.57	0.938
Thalamus left	4.72±0,46	4.74±0.73	0.939	4.61±0.5	4.59±0.63	0.937
Age	66.66±10.68	62.56±8.76	0.158	66.66±10.68	62.56±8.76	0.158

Table 2: Mean values of subcortical structures by gender in control group (cm^3), * p<0.05.

	Stereology			Semi-automatic segmentation		
	Female (n=11) (mean±SD)	Male (n=12) (mean±SD)	P value	Female (n=11) (mean±SD)	Male (n=12) (mean±SD)	P value
Caudate nucleus	4.43±0.86	4.42±0.82	0.975	4.43±0.67	4.45±0.63	0.967
Lentiform nucleus	7.19±1.23	7.83±1.003	0.186	7.28±0.85	7.56±0.92	0465
Thalamus	8.87±1.45	10.24±1.26	**0.025***	8.85±1.07	9.88±1.06	**0.031***

Stereological results

By the point-counting method using control subjects' MRI, the mean caudate nucleus, lentiform nucleus and thalamus volumes were 4.42±0.82, 7.52±1.14 and 9.59±1.49 cm^3, respectively. In patients with PD, these values were 3.78±0.89, 6.40±1.55 and 9.62±0.91 cm^3 respectively. Patients with PD had significantly smaller caudate nucleus and lentiform nucleus volumes than controls ($p<0.05$). However, no significant differences were determined between patients and control subjects for the volume of thalamus ($p>0.05$)**.** In addition, we calculated subcortical volumes according to the gender in control subjects. The mean (SD) caudate nucleus volumes were 4.42± 0.82 cm^3 in males, 4.43± 0.86 cm^3 in females, respectively. The mean values (SD) of lentiform nucleus and thalamus volumes were 7.83± 1.003 and 10.24± 1.26 cm^3 in males, 7.19 ± 1.23 and 8.87 ± 1.45 cm^3 in females, respectively. According to the statistical analysis, there was only a significant difference for thalamus volumes among the subjects with respect to gender ($p<0.05$) while no significant differences were detected for the other subcortical structures. The values obtained using stereology for each of the structure were given in Tables 1 and 2.

The mean CEs for volume estimation of caudate nucleus, lentiform nucleus and thalamus were under 5% (caudate nucleus 2.5%, lentiform nucleus 2.2%, and thalamus 2.1%).

Semi-automatic segmentation results

In control subjects, the mean values of caudate nucleus, lentiform nucleus and thalamus volumes by semi-automated segmentation method were 4.44±0.64, 7.43±0.87 and 9.35±1.13 cm^3, respectively. In patients with PD, these values were 3.92±0.94, 6.52±1.38 and 9.39±0.90 cm^3 respectively. According to the statistical analysis, caudate nucleus and lentiform nucleus volumes were calculated significantly smaller in patients with PD than controls ($p<0.05$). In addition to these, subcortical volumes were calculated and compared according to the gender in control subjects. Females had significantly smaller thalamus volumes than males ($p<0.05$), (Table 2). However, no significant differences was determined with respect to gender for the volume of caudate nucleus and lentiform nucleus ($p>0.05$)**.** The values

Table 3: Statistical method comparison values of subcortical structures in both two groups

	Control Group Streology-Segmentation		Parkinson's Group Streology-Segmentation	
	p value	r	p value	r
Caudate nucleus	0.864	0.793	0.073	0.954
Lentiform nucleus	0.352	0.915	0.114	0.977
Thalamus	0.141	0.923	0.08	0.843
Caudate nucleus right	0.749	0.869	0.058	0.945
Caudate nucleus left	0.950	0.650	0.229	0.934
Lentiform nucleus right	0.078	0.910	0.246	0.968
Lentiform nucleus left	0.942	0.897	0.115	0.968
Thalamus right	0.108	0.926	0.152	0.873
Thalamus left	0.051	0.891	0.102	0.762

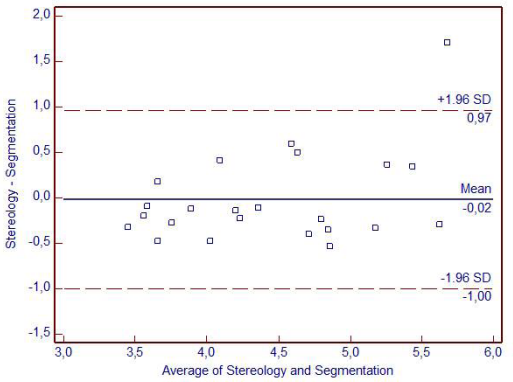

Figure 3. Bland–Altman analysis of the caudat nucleus volume as measured by semi-automated segmentation method versus point-counting technique in control group

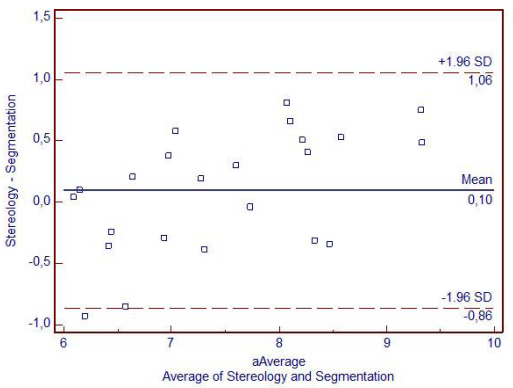

Figure 4. Bland–Altman analysis of the lentiform nucleus volume as measured by semi-automated segmentation method versus point-counting technique in control group

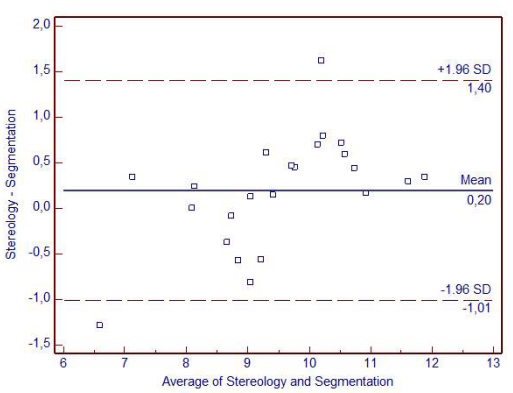

Figure 5. Bland–Altman analysis of the thalamus volume as measured by semi-automated segmentation method versus point-counting technique in control group

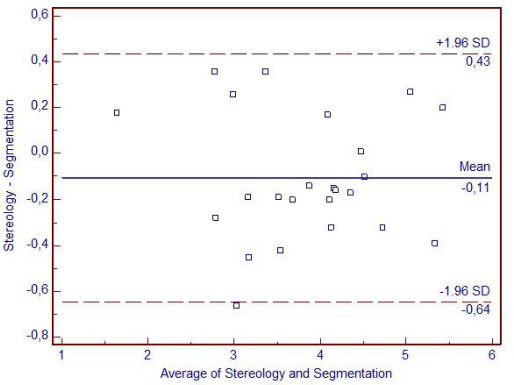

Figure 6. Bland–Altman analysis of the caudate nucleus volume as measured by semi-automated segmentation method versus point-counting technique in Parkinson's Group

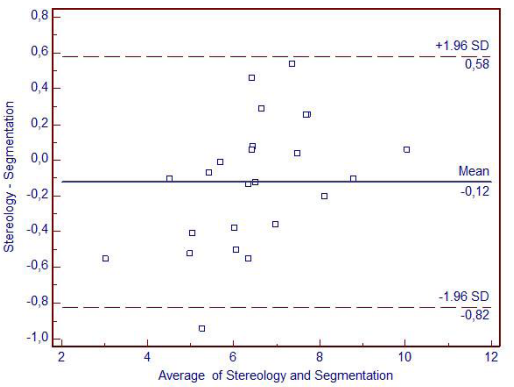

Figure 7. Bland–Altman analysis of the lentiform nucleus volume as measured by semi-automated segmentation method versus point-counting technique in Parkinson's Group

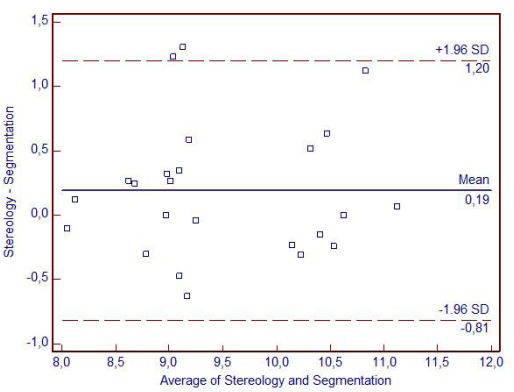

Figure 8. Bland–Altman analysis of the thalamus volume as measured by semi-automated segmentation method versus point-counting technique in Parkinson's Group

obtained using semi-automatic segmentation for each of the structure were given in Table 1.

Comparison of two methods with respect to subcortical brain structures' volume

The results of subcortical brain structures volumes, obtained using these two methods, were compared statistically. There was no difference between the caudate nucleus, lentiform nucleus and thalamus volume measurements obtained using the optimized point-counting technique and semi-automated segmentation in control subjects ($p>0.05$)**.** Similar results were obtained for patients with PD ($p>0.05$), (Table 3). Both methods showed a decrease in volume of caudate nucleus and lentiform nucleus in Parkinson's group compared to the control group.

The agreements between the stereology and segmentation methods were subjected to Bland-Altman plots using volume differences of 95. In control subjects, this showed that caudate nucleus, lentiform nucleus and thalamus volumes estimated by stereology and segmentation differed by between -1 and 0.97 cm^3, -0.86 and 1.06, -1.01 and 1.4 cm^3, respectively ($p>0.001$), (Figures 3-5). For patients with PD, these values differed by between -0.64 and 0.43 cm^3, -0.82 and 0.58, -0.81 and 1.20 cm^3 respectively (Figures 6-8). There was no significant difference between the two methods.

DISCUSSION

The subcortical brain structures' anomalies and volume changes were investigated using different methods and associated with various neurological and neuropsychiatric disorders such as Huntington's disease[10], Alzheimer's disease[7], PD[6] and frontotemporal lobar degeneration.[24] Therefore, a detailed anatomical knowledge of these disorders is necessary for early diagnosis and treatment.[25]

The accurate volume estimation of subcortical brain structures is an important process for the evaluation of brain disorders and abnormalities.[26,27] Quantitative analysis of regional brain atrophy and changes may be useful in differentiating PD from healthy controls and parkinsonian syndromes. In the last few years, several volumetric studies using reliable manual, semi-automated or fully-automated region of interest (ROI) techniques have been performed to characterize regional brain volume differences in parkinsonian degenerative disorders.[28-30] Structural changes in PD patients have been reported in cortical and subcortical areas. Regional atrophy has been observed in cortical areas including temporal, parietal and frontal lobes in PD patients compared to controls.[31,32]

Some of recent MRI-based volumetric studies directed to subcortical regions however, have reported conflicting results.[33-35] Menke *et al*.[33] segmented putamen, caudate, pallidum, thalamus, amygdala, and hippocampus from MRI of early-stage PD patients and control subjects. They reported no significant volumetric differences between PD patients and controls for any of the investigated structures. In one MR study, volumetric differences of subcortical structures in patients with PD were evaluated using fully-automated whole brain segmentation method. Caudate nucleus, putamen, pallidum and thalamus volumes were found to be 6.92, 9.34, 3.12 and 12.07 cm^3 in patients with PD respectively, while in controls 6.49, 9.01, 2.93 and 11.55 cm^3 respectively. There was no significant volumetric change in the relevant brain areas between patients with PD and healthy controls.[12]

Krabbe *et al*.[6] used tissue segmentation to analyze MRI from patients with PD and controls in order to measure regional volume changes. No significant correlation with age was found in any subcortical structure. In the putamen, there was however a trend towards negative correlation between age and volume. Caudate nucleus, putamen and thalamus volumes were found to be 6.55, 7.01 and 8.86 cm^3 in patients with PD respectively, while in controls 6.61, 8.13 and 8.44 cm^3, respectively. Putamen volume was significantly smaller in PD patients than in controls whereas no differences in caudate nucleus and thalamus volumes were found between PD patients and controls. In one MR study, caudate, putamen and thalamus volumes were significantly smaller in PD patients than in controls.[11] whereas no differences in putaminal volume were found between PD patients and controls in other studies.[36,37]

In one MRI study which aimed to delineate the specific locations of atrophy in striatal structures using a semiautomatic region-of-interest (ROI)-based approach determined that PD subjects had significantly lower scaled striatal volumes than control subjects. Average putamen volumes in PD subjects were 7.1% lower than controls, and caudate volumes were 7.0% lower. Subgroup analysis of PD subjects with shorter durations of disease (lowest 50% and lowest 25% compared to controls showed similar results).[35] Geevarghese *et al*.[38] studied the relationship between subcortical

structure volumes and clinical variables, such as age and motor severity scores in Parkinson's disease using segmentation method of MRI. They determined a correlation between volumes of the left and right thalamus and left and right putamen with increasing duration of disease. In addition, duration of symptoms was a significant factor relating to larger left thalamic volume. Male gender was also a significant factor associated with smaller left and right thalamic and right putaminal volumes. We determined a decrease in volume of caudate nucleus and lentiform nucleus in Parkinson's group compared to the control group. Our results by semi-automated segmentation and stereology are consistent with some researcher's results.[6,11,35]

In recent studies, the volumes of subcortical brain structures were estimated by some investigators using semi-automated image-processing procedures in healthy subjects.[6,39,40] Krabbe *et al*.[6] estimated the thalamus volume 8.44 cm^3 and Hokama *et al*.[40] estimated the globus pallidus volume 2.26 cm^3. Brambilla *et al*.[39] reported that the right and left caudate nucleus volumes were 2.38 ± 0.72, 2.71 ± 0.59, the right and left putamen volumes were 2.43 ± 0.93, 3.18 ± 0.92 and the right and left globus pallidus volumes were 1.53 ± 0.25 and 1.43 ± 0.17 cm^3 in healthy control subjects, respectively. Our results for control subjects using semi-automated segmentation and stereology methods are consistent with their results.

The subcortical regions were investigated in some disorders using stereology.[41,42] Vogels *et al*.[43] evaluated an efficient stereologic method for estimating the total volume of subcortical lesions and ventricular cerebrospinal fluid (CSF) volumes in patients with PD and to determine its accuracy and reproducibility. They reported coefficients of error of the individual volume estimates ranged from 0.01 to 0.13 and are negligible to the coefficients of the group mean (range, 0.70 to 0.89). For subcortical lesion volume, the random intraobserver error yielded 0.04 and for ventricular CSF 0.02; the random interobserver error amounted to 0.11 and 0.04, respectively; and the systematic interobserver error was 0.15 and 0.04, respectively. They reported that the stereologic method is sufficiently accurate, because the individual CEs are relatively negligible to the coefficient of variation of the group mean, constituting only a minor contribution to the total variation of the group mean. In addition to the radiological studies, in one study of the neuropathology of PD decreased density of striatal nerve cell populations was determined[44] whereas, no difference in striatal volumes or number of nerve cells between PD patients and controls was found in another.[45] There were no separate measures for putamen and caudate in these two studies. Neuropathology studies of the thalamus in PD have shown a non-significant nerve cell loss in the anterior paraventricular and anterior ventral lateral nuclei in PD.[46] Pederson *et al*.[47] compared total number of neocortical neurons between patients with PD and control subjects' brains using sterology technique. They determined no statistically significantly difference between groups. In addition, they reported any difference in the volume of white matter, central gray structures, archicortex, or the ventricular system between the two groups.

In some studies, the volume of brain tumor and lateral cerebral ventricles were calculated on MRIs using semi-automatic and manual methods and researchers determined any differences between the methods.[48,49] The hippocampus and total intracranial volume were studied using automatic, semi-automatic segmentation and manual tracing methods. The investigators concluded that there was a good correlation among the three methods.[50] In our previous study, we compared the volumes of subcortical brain structures and determine the probable volumetric asymmetry in healthy subjects using stereological (point counting) and semi-automatic segmentation methods. We did not find any significant differences among the subjects with respect to gender and no significant asymmetry in subcortical structures according to these methods. Also, no significant difference was found between point-counting and semiautomated segmentation methods for the volumes of subcortical structures. Our previous study was the first such study in healthy subjects.[9]

Thus, a patient group was added to the current study and we found that patients with PD had significantly smaller caudate nucleus and lentiform nucleus volumes than control, however no significant differences was determined between patients and control subjects for the volume of thalamus using both two methods. We did not find any significant difference between the two methods for subcortical structures.

Segmentation of subcortical structures in human brain MRI is an important and also a difficult task due to poor and variable-intensity contrast. Clear, well-defined intensity features are absent in many places along typical structure boundaries and an extra information is required to achieve successful segmentation.[51] However, the correct segmentation of subcortical structures for

studies of normal development and disease is still challenging.[52] Many factors may affect the MRI-derived automated morphometric measures. These factors are field strength such as different kinds of Tesla (1.5 vs. 3 T), scanner manufacturer such as different MRI manufacturer (Siemens vs. GE), pulse sequence (MPRAGE vs. multiple flip angle, multi-echo FLASH, etc.) and subject hydration status.[53,54] In addition, data processing-related factors, including not only software package and version, but also the parameters chosen for analysis may also affect measures.[55]

However, the evaluation of the accuracy of segmentation algorithms is more difficult because of the lack of a gold standard. Acer *et al*.[13,56] demonstrated that stereological results are very close to gold standard results in their studies. In addition, stereology method provides a coefficient of error (CE) of the measurement of the volume of the structure of interest. Therefore, it may be used to identify the optimal parameters of sampling needed to achieve a given precision such as we need the number of MRI sections and the density of the point grid. Thus, the stereological method provides an opportunity for the investigator making appropriate changes to their sampling or estimating procedures. If researchers obtain high CE, there are problems in accuracy of their results. So, they may change parameters of sampling (the spacing of points in the grid or the number of slices available in any MRI study) to provide a reasonable CE value.[57]

In conclusion, we demonstrated decresaing caudate and lentiform nucleus volumes in patients with PD. Detecting early signs and symptoms and developing biological markers for the preclinical diagnosis and progression of PD seem particularly important. MRI morphometry could be a potential biomarker in that regard. Our results indicate that the semi-automated segmentation and stereology methods can be used for reliable volume estimation of subcortical structures. The point-counting method is reliable, simple, inexpensive, and efficient method for estimating volumes in MRIs. For each subcortical structure, we found that counting 180–220 points on 16 or 20 systematically sampled MR sections with 1 mm section thickness and a point spacing of 0.4 cm enables volume estimation of subcortical structures with a CE below 5 %. To our knowledge, this is the first study to compare in vivo the regional brain volume changes in Parkinson's disease using stereological (point-counting) and semiautomated segmentation methods.

There are several limitations to our study. Our findings demonstrate that PD relates to volume changes of subcortical structures. These changes are likely to be multifactorial however, could be associated with pharmacological, pathological, and compensatory processes. We did not investigate the relationship between subcortical structure volumes and clinical variables, such as age and motor severity scores. Prospective studies are needed to ultimately clarify the relevance of subcortical volume changes in PD to better understanding the disease process and treatment option.

DISCLOSURE

Conflict of interest: None

REFERENCES

1. Brüggemann N, Külper W, Hagenah J, *et al*. Autosomal dominant Parkinson's disease in a large German pedigree. *Acta Neurol Scand* 2012; 126:129-37.
2. Braak H, Braak E. Pathoanatomy of Parkinson's disease. *J Neurol* 2000; 247:3-10.
3. De Jong LW, Van der Hiele K, Veer IM, *et al*. Strongly reduced volumes of putamen and thalamus in Alzheimer's disease: an MRI study. *Brain* 2008; 131:3277-85.
4. Gibb WR. Functional neuropathology in Parkinson's disease. *Eur Neurol* 1997; 38:21-5.
5. Gilbert AR, Rosenberg DR, Harenski K, Spencer S, Sweeney JA, Keshavan MS. Thalamic volumes in patients with first-episode schizophrenia. *Am J Psychiatry* 2001; 158:618-24.
6. Krabbe K, Karlsborg M, Hansen A, *et al*. Increased intracranial volume in Parkinson's disease. *J Neurol Sci* 2005; 239:45-52.
7. Kantarci K, Jack CR Jr. Quantitative magnetic resonance techniques as surrogate markers of Alzheimer's disease. *NeuroRx* 2004; 1:196-205.
8. Savoiardo M. Differential diagnosis of Parkinson's disease and atypical parkinsonian disorders by magnetic resonance imaging. *Neurol Sci* 2003; 24:35-7.
9. Ertekin T, Acer N, Içer S, Ilıca AT. Comparison of two methods for the estimation of subcortical volume and asymmetry using magnetic resonance imaging: a methodological study. *Surg Radiol Anat* 2013; 35:301-9.
10. Douaud G, Gaura V, Ribeiro MJ, *et al*. Distribution of grey matter atrophy in Huntington's disease patients: a combined ROI based and voxel based morphometric study. *Neuroimage* 2006; 32:1562-75.
11. Lisanby SH, McDonald WM, Massey EW, *et al*. Diminished subcortical nuclei volumes in Parkinson's disease by MR imaging. *J Neural Transm Suppl* 1993; 40:13-21.
12. Messina D, Cerasa A, Condino F, *et al*. Patterns of brain atrophy in Parkinson's disease, progressive supranuclear palsy and multiple system atrophy. *Parkinsonism Relat Disord* 2011; 17:172-6.

13. Acer N, Bayar B, Basaloglu H, Oner E, Bayar K, Sankur S. Unbiased estimation of the calcaneus volume using the Cavalieri principle on computed tomography images. *Ann Anat* 2008; 190:452-60.
14. Gundersen HJ, Jensen EB. The efficiency of systematic sampling in stereology and its prediction. *J Microsc* 1987; 147:229-63.
15. Mayhew TM, Olsen DR. Magnetic resonance imaging (MRI) and model-free estimates of brain volume determined using the Cavalieri principle. *J Anat* 1991; 178:133-44.
16. Acer N, Sahin B, Usanmaz M, Tato4u H, Irmak Z. Comparison of point counting and planimetry methods for the assessment of cerebellar volume in human using magnetic resonance imaging: a stereological study. *Surg Radiol Anat* 2008; 30:335-9.
17. Cruz-Orive LM. A general variance predictor for Cavalieri slices. *J Microsc* 2006; 222:158-65.
18. Ertekin T, Acer N, Turgut AT, Aycan K, Ozçelik O, Turgut M. Comparison of three methods for the estimation of the pituitary gland volume using magnetic resonance imaging: a stereological study. *Pituitary* 2011; 14:31-8.
19. Sahin B, Ergur H. Assessment of the optimum section thickness for the estimation of liver volume using magnetic resonance images: a stereological gold standard study. *Eur J Radiol* 2006; 57:96-101.
20. Gonzalez RC, Woods RE, Eddins SL. Digital image processing using Matlab. 1st Ed. Upper Saddle River (NJ): Prentice Hall; 2004:55-87.
21. Jung C, Kim C. Segmenting clustered nuclei using H-minima transform-based marker extraction and contour parameterization. *IEEE Trans Biomed Eng* 2010; 57:2600-4.
22. Saleh MD, Eswaran C. An efficient algorithm for retinal blood vessel segmentation using h-maxima transform and multilevel thresholding. *Comput Methods Biomech Biomed Engin* 2012; 15:517-25.
23. Canny J. A computational approach to edge detection. *IEEE Trans Pattern Anal Mach Intell* 1986; 8:679-98.
24. Looi JC, Lindberg O, Zandbelt BB. Caudate nucleus volumes in frontotemporal lobar degeneration: Differential atrophy in subtypes. *AJNR Am J Neuroradiol* 2008; 29:1537-43.
25. Mamah D, Wang L, Barch D, de Erausquin GA, Gado M, Csernansky JG. Structural analysis of the basal ganglia in schizophrenia. *Schizophr Res* 2007; 89:59-71.
26. Filipek PA, Kennedy DN, Caviness VS. Volumetric analyses of central nervous system neoplasm based on MRI. *Pediatr Neurol* 1991; 7:347-51.
27. Shenton ME, Kikinis R, Jolesz FA, *et al*. Abnormalities of the left temporal lobe and thought disorder in schizophrenia: a quantitative magnetic resonance imaging study. *N Eng J Med* 1992; 327:604-12.
28. Paviour DC, Price SL, Jahanshahi M, Lees AJ, Fox NC. Longitudinal MRI in progressive supranuclear palsy and multiple system atrophy: rates and regions of atrophy. *Brain* 2006; 129:1040-9.
29. Paviour DC, Price SL, Jahanshahi M, Lees AJ, Fox NC. Regional brain volumes distinguish PSP, MSA-P, and PD: MRI-based clinico-radiological correlations. *Mov Disord* 2006; 21:989-96.
30. Tinaz S, Courtney MG, Stern CE. Focal cortical and subcortical atrophy in early Parkinson's disease. *Mov Disord* 2011; 26:436-41.
31. Summerfield C, Junque C, Tolosa E, et al. Structural brain changes in Parkinson disease with dementia: a voxel-based morphometry study. *Arch Neurol* 2005; 62:281-5.
32. Cordato NJ, Duggins AJ, Halliday GM, Morris JG, Pantelis C. Clinical deficits correlate with regional cerebral atrophy in progressive supranuclear palsy. *Brain* 2005; 128:1259-66.
33. Menke RA, Szewczyk-Krolikowski K, Jbabdi S, *et al*. Comprehensive morphometry of subcortical grey matter structures in early-stage Parkinson's disease. *Hum Brain Mapp* 2014; 35:1681-90.
34. Quattrone A, Nicoletti G, Messina D, *et al*. MR imaging index for differentiation of progressive supranuclear palsy from Parkinson disease and the Parkinson variant of multiple system atrophy. *Radiology* 2008; 246:214-21.
35. Sterling NW, Du G, Lewis MM, et al. Striatal shape in Parkinson's disease. *Neurobiol Aging* 2013; 34:2510-6.
36. Brenneis C, Seppi K, Schocke MF, *et al*. Voxel-based morphometry detects cortical atrophy in the Parkinson variant of multiple system atrophy. *Mov Disord* 2003; 18:1132-8.
37. Schrag A, Kingsley D, Phatouros C, *et al*. Clinical usefulness of magnetic resonance imaging in multiple system atrophy. *J Neurol Neurosurg Psychiatry* 1998; 65:65-71.
38. Geevarghese R, Lumsden DE, Hulse N, Samuel M, Ashkan K. Subcortical structure volumes and correlation to clinical variables in Parkinson's Disease. *J Neuroimaging* 2014. doi: 10.1111/jon.12095. [Epub ahead of print]
39. Brambilla P, Harenski K, Nicoletti MA *et al*. Anatomical MRI study of basal ganglia in bipolar disorder patients. *Psychiatry Res* 2001; 106:65-80.
40. Hokama H, Shenton ME, Nestor PG, *et al*. Caudate, putamen, and globus pallidus volume in schizophrenia: a quantitative MRI study. *Psychiatry Res* 1995; 61:209-29.
41. Hallahan BP, Craig MC, Toal F, *et al*. In vivo brain anatomy of adult males with Fragile X syndrome: an MRI study. *Neuroimage* 2011; 54:16-24.
42. Kreczmanski P, Heinsen H, Mantua V *et al*. Volume, neuron density and total neuron number in five subcortical regions in schizophrenia. *Brain* 2007; 130:678-92.
43. Vogels OJ, Zijlmans JC, Van't Hof MA, Thijssen HO, Horstink MW. MR volume estimation of subcortical brain lesions and ventricular cerebrospinal fluid: A simple and accurate stereologic method. *AJNR Am J Neuroradiol* 1995; 16:1441-5.
44. Bugiani O, Perdelli F, Salvarani S, Leonardi A, Mancardi GL. Loss of striatal neurons in Parkinson's disease: a cytometric study. *Eur Neurol* 1980; 19:339-44.
45. Bottcher J. Morphology of the basal ganglia in Parkinson's disease. *Acta Neurol Scand* 1975; 62:1-87.
46. Xuereb JH, Perry RH, Candy JM, Perry EK, Marshall E, Bonham JR. Nerve cell loss in the thalamus in Alzheimer's disease and Parkinson's disease. *Brain* 1991; 114:1363-79.

47. Pedersen KM, Marner L, Pakkenberg H, Pakkenberg B. No global loss of neocortical neurons in Parkinson's disease: a quantitative stereological study. *Mov Disord* 2005; 20:164-71.
48. Calmon G, Roberts N. Automatic measurement of changes in brain volume on consecutive 3D MR images by segmentation propagation. *Magn Reson Imaging* 2000; 18:439-53.
49. Xie K, Yang J, Zhang ZG, Zhu YM. Semi-automated brain tumor and edema segmentation using MRI. *Eur J Radiol* 2005; 56:12-9.
50. Ishii K, Soma T, Kono AK, et al. Automatic volumetric measurement of segmented brain structures on magnetic resonance imaging. *Radiat Med* 2006; 24:422-30.
51. Patenaude B, Smith SM, Kennedy DN *et al*. A Bayesian model of shape and appearance for subcortical brain segmentation. *Neuroimage* 2011; 56:907-22.
52. Wonderlick JS, Ziegler DA, Hosseini-Varnamkhasti P *et al*. Reliability of MRI-derived cortical and subcortical morphometric measures: effects of pulse sequence, voxel geometry, and parallel imaging. *Neuroimage* 2009; 44:1324-33.
53. Han X, Jovicich J, Salat D, *et al*. Reliability of MRI-derived measurements of human cerebral cortical thickness: The effects of field strength, scanner upgrade and manufacturer. *Neuroimage* 2006; 32:180-94
54. Jovicich J, Czanner S, Greve D *et al*. Reliability in multisite structural MRI studies: effects of gradient non-linearity correction on phantom and human data. *Neuroimage* 2006; 30:436-43.
55. Jovicich J, Czanner S, Han X, *et al*. MRI-derived measurements of human subcortical, ventricular and intracranial brain volumes: Reliability effects of scan sessions, acquisition sequences, data analyses, scanner upgrade, scanner vendors and field strengths. *Neuroimage* 2009; 46:177-92.
56. Acer N, Sofikerim M, Ertekin T, Unur E, Çay M, Öztürk F. Assessment of in vivo calculation with ultrasonography compared to physical sections in vitro: A stereological study of prostate volumes. *Anat Sci Int* 2011; 86:78-85.
57. Sahin B, Emirzeoglu M, Uzun A, *et al*. Unbiased estimation of the liver volume by the Cavalieri principle using magnetic resonance images. *Eur J Radiol* 2003; 47:164-70.